Cancer Cell
Article

A Human ICAM-1 Antibody Isolated by a Function-First Approach Has Potent Macrophage-Dependent Antimyeloma Activity In Vivo

Niina Veitonmäki,[1,5,6] Markus Hansson,[2,5] Fenghuang Zhan,[3] Annika Sundberg,[1] Tobias Löfstedt,[1] Anne Ljungars,[1] Zhan-Chun Li,[1] Titti Martinsson-Niskanen,[1] Ming Zeng,[4] Ye Yang,[3] Lena Danielsson,[1] Mathilda Kovacek,[1] Andrea Lundqvist,[1] Linda Mårtensson,[1] Ingrid Teige,[1] Guido Tricot,[3] and Björn Frendéus[1,*]

[1]BioInvent International, Sölvegatan 41, 22370 Lund, Sweden
[2]Department of Hematology, BMC 13, Skåne University Hospital, Lund University, 221 84 Lund, Sweden
[3]Division of Hematology, Oncology, and Blood and Marrow Transplantation, Department of Internal Medicine, University of Iowa, Iowa City, IA 52242, USA
[4]School of Public Health, Central South University, 110 Xiangya Road, Changsha, Hunan 410078, PR China
[5]These authors contributed equally to this work
[6]Present address: Alligator Bioscience, 223 81 Lund, Sweden
*Correspondence: bjorn.frendeus@bioinvent.com
http://dx.doi.org/10.1016/j.ccr.2013.02.026

SUMMARY

We isolated a tumor B-cell-targeting antibody, BI-505, from a highly diversified human phage-antibody library, using a pioneering "function-first" approach involving screening for (1) specificity for a tumor B cell surface receptor, (2) induction of tumor programmed cell death, and (3) enhanced in vivo antitumor activity compared to currently used treatments. BI-505 bound to intercellular adhesion molecule-1, identifying a previously unrecognized role for this receptor as a therapeutic target in cancer. The BI-505 epitope was strongly expressed on the surface of multiple myeloma cells from both newly diagnosed and relapsed patients. BI-505 had potent macrophage-dependent antimyeloma activity and conferred enhanced survival compared to currently used treatments in advanced experimental models of multiple myeloma.

INTRODUCTION

Targeted immunotherapy plays an increasingly important role in the treatment of cancer (Weiner et al., 2010). Still, antibodies with antitumor activity have yet to be generated for several types of cancer, and a significant proportion of patients who initially respond to the currently available therapies develop resistance (Smith, 2003). The search for antitumor antibodies is thus critical for the further development of targeted immunotherapy.

A common first step of conventional antibody discovery approaches is to isolate antibodies with specificity for a predefined target structure, which may be previously uncharacterized or well validated with respect to cancer therapy. Therapeutic efficacy is not, however, easily predicted from antibody target specificity; antibodies to the same target receptor may vary greatly in therapeutic efficacy independent of their binding affinity (Beers et al., 2008; Cragg and Glennie, 2004), and antibodies against alternative molecular targets may show promising, and sometimes unexpected, therapeutic potential (Beck et al., 2010; Cheson and Leonard, 2008). It is therefore important to use a "function-first," rather than a target specificity-based, approach to therapeutic antibody discovery.

We have developed an approach that allows screening of large numbers of antibodies for useful antitumor activity without prior identification of the target receptors (Fransson et al., 2006). This high-throughput, function-first approach allows rapid identification of candidates that display key properties for an antitumor antibody, e.g., specificity for differentially expressed

Significance

Antibody therapy plays a growing role in the treatment of cancer. Antibodies may exert their therapeutic function by targeting ligand-receptor signaling pathways and/or by triggering of antibody-unique effector functions. Here, we describe potent in vivo antimyeloma activity of an antibody isolated by target-unbiased functional screening for tumor cell death. Mechanism-of-action studies demonstrated that the antibody induced apoptosis in target tumor cells and activated macrophage-dependent host antitumor immunity in a manner that would not have been predicted from currently available information on the receptor targeted by the antibody. Our results help illustrate how functional screening may complement predefined target approaches to broaden therapeutic target space by discovering functions of known targets.

tumor cell surface receptors, significant ability to confer programmed cell death (PCD) in tumors, and significant antitumor activity in vivo compared to currently used treatments.

When applied to find antibodies with improved antitumor activity against B cell malignancies, the process identified several tumor PCD-inducing antibodies—specific for different tumor B-cell-associated receptors—that showed better antitumor activity compared to rituximab, a CD20-specific monoclonal antibody used for treatment of CD20-expressing B cell cancers (Fransson et al., 2006).

Interestingly, among antibodies identified were several specific for intercellular adhesion molecule 1 (ICAM-1), a receptor not previously associated with tumor PCD. ICAM-1 is highly expressed in several human malignancies and is believed to be involved in their pathogenesis (Aalinkeel et al., 2004; Hideshima et al., 2007; Huang et al., 1995; Johnson et al., 1988; Schmidmaier et al., 2006). Notably, ICAM-1 was recently reported to be overexpressed and associated with advanced disease and poor survival in multiple myeloma (MM) (Sampaio et al., 2009; Schmidmaier et al., 2006). Further, evidence suggests that ICAM-1 is upregulated and causally related to MM patient development of resistance to chemotherapy (Sampaio et al., 2009; Schmidmaier et al., 2006; Zheng et al., 2009). ICAM-1, by binding to integrin β2 receptors and muc-1, is involved in cell-adhesive events that trigger multiple cell-signaling pathways promoting MM cell proliferation, migration, resistance to apoptosis, and development of cell adhesion molecule-induced drug resistance (Hideshima et al., 2007; Schmidmaier et al., 2004; Zheng et al., 2009). There is no curative treatment for MM, and the currently available therapy is associated with significant toxicity and development of drug resistance (Kyle and Rajkumar, 2004). MM plasma cells typically do not express the B cell antigen CD20 or show low and heterogeneous CD20 expression, making CD20-targeted therapies ineffective in this disease (Kapoor et al., 2008; Richardson et al., 2011).

Here, we characterize MM plasma cells for expression of the ICAM-1 epitope targeted by our function-first-isolated antibody BI-505, and we investigate BI-505's therapeutic activity and mechanism-of-action in well-established experimental models of MM.

RESULTS

A Human ICAM-1 Antibody Isolated by a Function-First Approach Has Significant Antitumor Activity against B Cell Cancer Xenografts

We isolated multiple antibodies inducing programmed cell death (PCD) in B cell lymphomas, targeting different tumor-cell-associated surface receptors, by means of a sequential process involving differential biopanning and high-throughput PCD screening of antibodies from the n-CoDeR (Söderlind et al., 2000) human antibody library (Figures S1A–S1C available online). The high specificity for ICAM-1 of one of these antibodies, BI-505 (appears as B11 in Fransson et al., 2006), is shown in Figure S1C. BI-505 dose-dependently induced PCD in ICAM-1-expressing Ramos, Raji, and Daudi lymphoma cells (Fransson et al., 2006; Figure 2D).

In order to further investigate the therapeutic potential of PCD-inducing ICAM-1 antibodies, we screened BI-505 for in vivo antitumor activity in tumor models comprising SCID mice transplanted with the lymphoblastic cell lines ARH-77 or Daudi. Both cell lines express the CD20 antigen, making it possible to compare antitumor efficacy and potency of antibodies identified here with those of the clinically validated CD20-specific monoclonal antibody rituximab.

Subcutaneous injection of ARH-77 cells resulted in rapid establishment and growth in SCID mice, with tumors being readily palpable between 12 and 14 days. Twice-weekly injections of 20 mg/kg of BI-505 commencing 1 day after tumor cell inoculation prevented tumor growth in 9 out of 10 injected mice (Figure 1A). Rituximab conferred significant antitumor activity at the same dose but was less efficacious than BI-505 (Figure 1A). Furthermore, BI-505 administered at a 100 times lower dose (0.2 mg/kg) was equally efficacious compared to 20 mg/kg rituximab in conferring survival (Figure 1B). The high efficacy and potency of BI-505 was confirmed in mice carrying ARH-77 tumors established for 12 days before the start of antibody treatment (Figures 1C and 1D). In this model, rituximab failed to reduce tumor growth or promote animal survival ($p > 0.05$), whereas BI-505 both significantly reduced tumor growth (Figure 1C; $p < 0.05$) and prolonged animal survival (Figure 1D; $p < 0.05$). Thus, in this aggressive model of CD20-positive B cell malignancy, BI-505 was more efficacious and more potent in conferring antitumor activity and survival than rituximab.

We also tested BI-505's antitumor activity against Daudi B cell lymphoma xenografts. Again, BI-505 significantly prevented tumor growth (Figures 1E and 1G; $p < 0.001$) and prolonged survival (Figures 1F and 1H; $p < 0.001$) of tumor-bearing mice when administered 1 day following tumor cell injection (Figures 1E and 1F) or when established tumors were treated (Figures 1G and 1H), this time with equal efficacy compared to rituximab (Figures 1E–1H). The overall stronger antitumor activity of BI-505 compared with rituximab was not caused by a higher number of tumor cell epitopes for BI-505 than for rituximab. In contrast, flow cytometric analysis revealed that both ARH-77 (Figure 1I) and Daudi (Figure 1J) cells expressed significantly fewer BI-505 epitopes than rituximab epitopes, and immunohistochemical analysis of tumor tissue harvested from mice treated with BI-505, rituximab, or isotype control antibodies showed that tumors expressed both rituximab and BI-505 epitopes at the completion of experimentation (Figure S1D).

To establish the potency of BI-505 in vivo and the lowest dose achieving maximal antitumor activity, we performed a dose-titration experiment using the SCID/ARH-77 model system. BI-505 showed dose-dependent antitumor activity, which followed a sigmoidal curve, peaking at the 2 mg/kg dose and remaining near maximal at a dose of 0.2 mg/kg (Figures 2A and 2B). Antibody concentrations in mouse sera were determined by ELISA and were plotted as a function of maximal in vivo antitumor activity (Figure 2C). The relationship between BI-505 concentration-dependent in vivo antitumor activity, in vitro antitumor (PCD) activity (Figure 2D), and in vitro receptor occupancy (Figure 2E) was then examined by overlaying generated curves in a single graph (Figure 2F). BI-505 concentration-dependent receptor occupancy correlated nearly perfectly with BI-505 in vitro and in vivo antitumor activity (Figure 2F). This result is consistent with ICAM-1-dependent direct cell cytotoxicity underlying BI-505's antitumor activity.

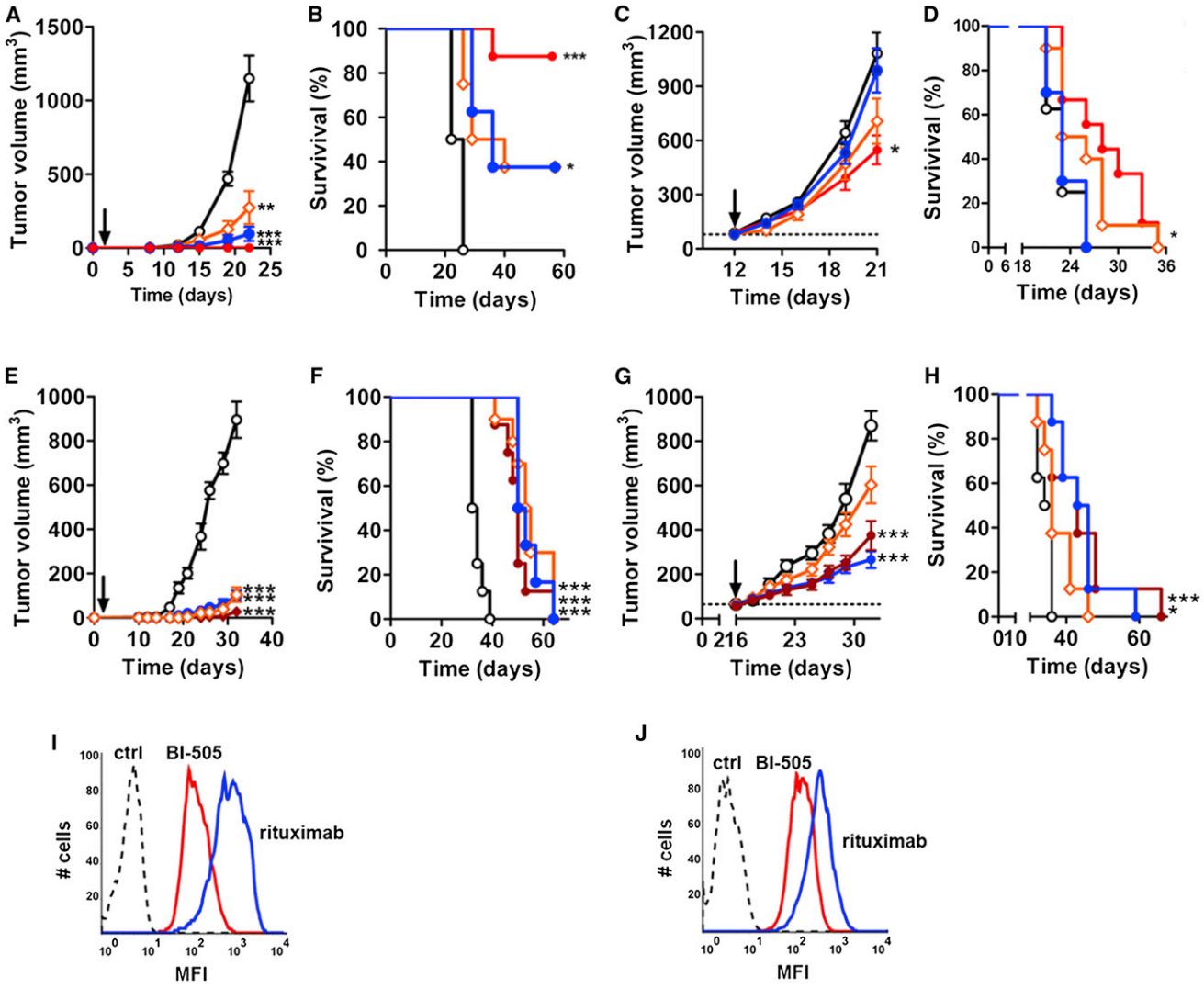

Figure 1. BI-505 Has Significant In Vivo Antitumor Activity against CD20-Expressing Tumors Compared with Rituximab

(A–H) Mean tumor volumes (A, C, E, and G) and survival (B, D, F, and H) of mice xenografted with CD20-expressing ARH-77 (A–D) or Daudi (E–H) cells and treated with BI-505 (bright red line = 20 mg/kg BI-505; maroon line = 2 mg/kg BI-505; and orange line = 0.2 mg/kg BI-505), rituximab (20 mg/kg, blue line), or isotype control (20 mg/kg, black line) antibodies in prophylactic (A, B, E, and F) or established (C, D, G, and H) tumor models. There were eight to ten animals per treatment/dose group. Tumor cells were injected day 0, and antibody treatment started as indicated in the graphs (black arrow). *$p < 0.05$, **$p < 0.01$, and ***$p < 0.001$. Error bars show ± SD. (I and J) FACS analysis of BI-505 and rituximab epitopes on the surface of ARH-77 (I) and Daudi (J) tumor cells. Antibodies were used at binding saturating concentrations.

See also Figure S1.

We conclude that BI-505 confers potent and direct antitumor activity against different types of B cell cancer.

ICAM-1 and the BI-505 Epitope Are Strongly Expressed in Multiple Myeloma

We next evaluated expression of the BI-505 epitope on bone marrow cells in patients with MM and related diseases (plasmacytoma, plasma cell leukemia, and light-chain amyloidosis) by flow cytometry (Figure 3; Table 1). Myeloma cells were identified using fluorescent antibodies against surface antigens CD38, CD138, CD45, and CD56 (Figure S2A), according to the European Myeloma Network guidelines on multiparametric flow cytometry in MM (Rawstron et al., 2008) and confirming monoclonal MM cells with intracellular staining of λ and κ light chains. All MM patients expressed the BI-505 epitope on most (97% ± 4%, mean ± SD, patient n = 22) myeloma cells (Figure 3; Table 1). The BI-505 epitope was generally very highly expressed on these cells, with a median expression level that was ten times higher than on normal B cells from the same patients. Similar results were obtained with a commercially available anti-ICAM-1 antibody (data not shown). Furthermore, the BI-505 epitope was highly expressed on myeloma cells in a patient in relapse who had received several different lines of therapy (Figure S2B). Thus, ICAM-1 and the BI-505 epitope are strongly expressed on the surface of MM plasma cells.

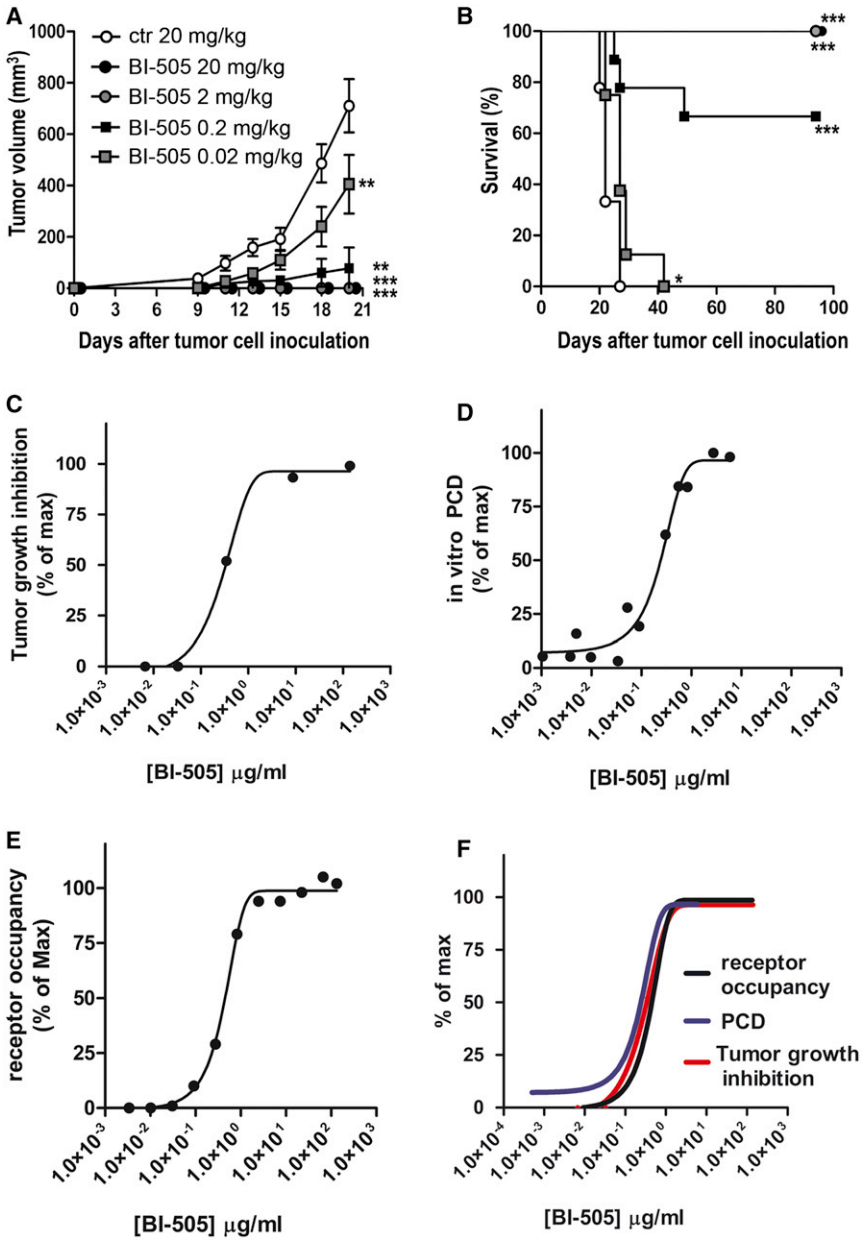

Figure 2. BI-505 Dose-Dependent Antitumor Activity Correlates with ICAM-1 Receptor Occupancy on Tumor Cell Surfaces

(A and B) Mean tumor volumes (A) and mean survival (B) of mice treated with different doses of BI-505 in the ARH-77 tumor model. Error bars show ± SD. *$p < 0.05$, **$p < 0.01$, and ***$p < 0.001$. (C–E) BI-505 concentration-dependent in vivo antitumor activity (C), in vitro antitumor (tumor PCD) activity (D), and receptor occupancy of tumor cell-expressed ICAM-1 (E).

(F) A combined plot of (C)–(E). There were eight to ten animals per treatment group.

BI-505 Has Broad Antimyeloma Activity In Vivo

Because we found high expression of the BI-505 epitope in human MM, we proceeded to screen BI-505 for in vivo antimyeloma activity using SCID/xenograft models comprising four well-characterized MM cell-lines. These cell lines express the myeloma markers CD38 and CD138 but do not express CD20. Twice-weekly dosing with 2 mg/kg of BI-505 starting 1 day after tumor cell injection reduced myeloma tumor growth in mice xenografted with ICAM-1-expressing cell lines EJM, RPMI-8226, and NCI-H929 by 98%, 96%, and 99%, respectively (Figures 4A and 4B). In contrast, BI-505 did not affect tumor growth in mice xenografted with the ICAM-1-negative cell line OPM-2 (Figures 4A and 4B). Taken together, these studies indicated that BI-505 had highly efficacious, broad, and ICAM-1-dependent in vivo antimyeloma activity.

BI-505 Has Potent Antimyeloma Activity in Clinically Relevant Models of Advanced Myeloma

To assess the therapeutic potential of BI-505 for treatment of MM, we next compared the antimyeloma effects of BI-505 to current gold-standard treatment in disseminated experimental models of MM sharing characteristics with human disease. These models resemble the manifestation and progression of human MM disease in many respects, including tumor dissemination and establishment in bone marrow, and the appearance of osteolytic bone lesions and hypercalcemia (Mitsiades et al., 2003; Yaccoby et al., 1998). First, we compared the antimyeloma activity of BI-505 with currently used treatments in an advanced disseminated MM model comprising RPMI-8226 myeloma cells. In this model, therapeutic treatment with 2 mg/kg BI-505 was started 5 days after intravenous grafting of MM cells to allow for homing and establishment of MM cells in bone marrow. BI-505 significantly enhanced survival and delayed disease onset compared to treatment with the comparator drugs bortezomib, lenalidomide, melphalan, or dexamethasone (Figure 5A), all approved and currently used for MM therapy. Importantly, Figure 5A shows the effect of the comparator drugs used at maximally efficacious, and clinically relevant, doses. Higher doses of some of the comparator drugs were shown to be toxic, but not more efficacious, to animals (data not shown).

Primary human MM cells depend on interactions with bone marrow stromal cells to proliferate and survive. The SCID-hu mouse harbors a human microenvironment, where primary patient MM cells proliferate and induce pathology similar to human clinical MM (Yaccoby et al., 1998). MM-cell-derived human immunoglobulin G (IgG) titers were detected (>10 μg/ml) in the serum of SCID-hu mice 4 weeks after implantation of human MM cells to transplanted human bones, at which time treatment with antibodies (2 mg/kg) or bortezomib (1 mg/kg) began. Human IgG titers increased steadily in control-treated SCID-hu

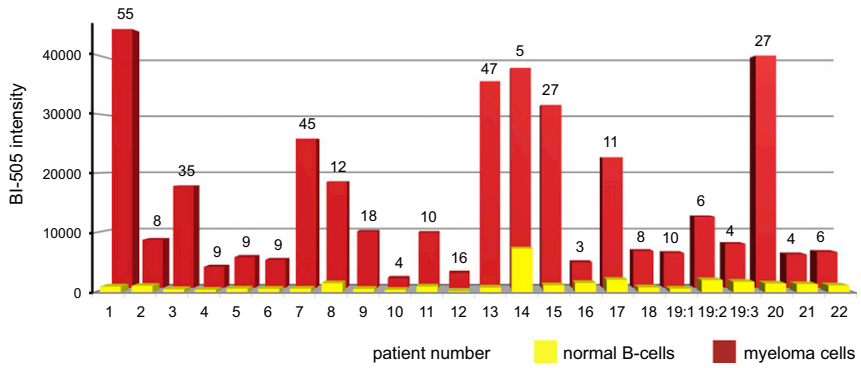

Figure 3. The BI-505 Epitope Is Highly Expressed on the Surface of Primary MM Plasma Cells

FACS analysis of BI-505 epitope expression on the cell surface of patients' MM cells (red bars) versus normal B cells (yellow bars). Numbers on top of bars indicate fold increase of the BI-505 epitope on surface of MM cells compared to normal B cells. Patient numbers correspond to those shown in Table 1.

See also Figure S2.

mice over the course of experimentation to reach maximal concentrations of 40 ± 5 μg/ml just before sacrifice (Figures 5B and S3). In contrast, therapeutic treatment with BI-505 or bortezomib halted or reduced serum human IgG levels to below pretreatment levels ($hIgG_{BI\text{-}505}$ = 91% ± 22%), demonstrating a significant anti-MM effect. Two independent experiments were performed with similar results (Figures 5B and S3), each with MM cells from two different patient donors (n = 4). Immunohistochemical staining for human CD138-expressing cells in harvested human bone implants indicated that BI-505 antimyeloma effects correlated with decreased tumor burden (Figure 5C). BI-505 antimyeloma effects correlated with protection against MM-induced bone pathology as demonstrated by decreased bone remodeling with decreased loss of bone mineral density (Figure 5D). Staining of a limited number of bone sections indicated reduced numbers of bone osteoclasts (Figure 5E) and total infiltrated nucleated cells (Figure 5F) in BI-505- or bortezomib-treated mice compared to control-treated mice.

Thus, in two clinically relevant experimental models BI-505 anti-MM activity was equal to or greater than currently available drugs.

BI-505 Confers Fc-FcγR-Dependent Antitumor Activity through Macrophages

Previous studies have demonstrated PCD-inducing properties of BI-505 in a wide range of tumor B cell lines (Fransson et al., 2006). BI-505 PCD was enhanced by antibody crosslinking in vitro, indicating that in vivo antitumor activity might be enhanced by crosslinking provided by FcγR-expressing cells (Wilson et al., 2011). Given the critical importance of FcγR-mediated antitumor mechanisms for the clinical and in vivo therapeutic activity of clinically validated cancer mAbs (Clynes et al., 2000; Musolino et al., 2008; Weng and Levy, 2003), we addressed the contribution of antibody Fc: host FcγR-dependent mechanisms for BI-505's therapeutic activity. To this end, we engineered BI-505 variants with abolished ($IgG_{1\ N297Q}$, "Fc-mut"), or reduced (BI-505-IgG_4) FcγR-binding compared to wild-type BI-505 IgG_1, and investigated their respective in vivo therapeutic activities. The Fc-switch variants retained affinities for ICAM-1 as evidenced by near identical EC_{50} values for binding to recombinant or cell-surface-expressed ICAM-1 (Figures S4A–S4C). The in vivo antitumor activity of BI-505 Fc-variants (Figure 6A) correlated perfectly with binding to mouse FcγRIV (Figure 6B)—the structural and functional homolog of human FcγRIIIa and a principal murine FcγR conferring antibody-mediated cell cytotoxicity in vivo (Nimmerjahn et al., 2005)—increasing in the order of $IgG_{1\ N297Q} < IgG_4 < IgG_1$. Importantly, mice treated with IgG_1, IgG_4, and $IgG_{1\ N297Q}$ variant antibodies of BI-505 had similar serum antibody titers at the end of experimentation, indicating that the different antibody variants had similar in vivo half-lives and demonstrating that differential antitumor activity did not result from differential pharmacokinetics (Table S1). These findings demonstrated that BI-505 in vivo antitumor activity was Fc: FcγR-dependent.

Fc-FcγR-interactions, in addition to enhancing antibody-induced negative signaling and tumor PCD (Wilson et al., 2011), may involve both innate and adaptive arms of cellular immunity (Alduaij and Illidge, 2011; Park et al., 2010). We used different approaches to assess the role of NK cells and macrophages—two principal cell types capable of conferring FcγR-dependent antitumor effects—for BI-505 therapeutic activity. First, we examined the relative abundance of these cell types in tumor tissue harvested from BI-505 or control-antibody-treated mice. By immunohistochemistry, we found that macrophages ($F4/80^+$ cells) constituted the vast majority of FcγR-expressing cells in BI-505-treated tumors (Figure 6D). In contrast, very few intratumoral NK cells could be detected ($CD49b^+$ $CD31^-$ cells). Furthermore, and interestingly, treatment with BI-505 significantly increased tumor macrophage infiltration but—conversely—decreased tumor NK cell content (Figure 6D). Together, these data suggested that macrophages, but not NK cells, were principal FcγR-expressing cells conferring BI-505 antitumor activity in vivo. To verify this, we depleted macrophages or NK cells, using clodronate liposomes and anti-asialo antibodies, respectively, from SCID mice bearing established RPMI-8226 myeloma tumors and examined the effect on BI-505 antimyeloma activity. A period of 3 weeks of macrophage and NK cell depletion was chosen as readout because this was the longest time period in which neither treatment affected animal well-being. Cell depletion did not per se impact tumor growth over this period of time (Figures S4D and S4E). Figure 6E clearly demonstrates that macrophage depletion completely abolished BI-505 in vivo antitumor activity. Tumors of macrophage depleted BI-505-treated mice had doubled in size compared with tumors from animals receiving BI-505 treatment alone ($V_{BI\text{-}505}$ = 95 ± 39 mm^3, $V_{BI\text{-}505+clodro}$ = 189 ± 94 mm^3, $p < 0.001$) but were similarly sized compared to tumors from control-antibody-treated mice ($V_{ctrl\ IgG}$ = 198 ± 90 mm^3, $p > 0.05$). NK cell depletion, in contrast, had little or no effect on BI-505 antitumor activity. Tumor volumes of NK-cell-depleted

Table 1. Expression of the BI-505 Epitope in a Cohort of 29 Patients with Plasma Cell Disorders

Patient Characteristics										BI-505 Epitope Expression	
Patient Number[a]	Age (year)	Sex[b]	Ig[c]	M- comp (g/l)	Skel. Dest[d] (n)	MM Cells[e] (%)	ISS[f]	T[g] (n)	Diagnosis[h]	Intensity[i]	Positive Cells (%)
1	38	m	IgG	10	0	14	I	0	MM	+++	98
2	46	m	IgG	38	0	34	II	0	MM	+++	97
3	53	f	IgG	14	>10	6	I	0	MM	+++/++	100
4	54	m	–	–	3	22	III	2	nsMM	+++	100
5	59	m	IgG	32	>10	29	I	0	MM	++	100
6	60	f	IgG	4	3	2	II	1	MM	+++	98
7	60	f	IgA	26	1	10	I	0	MM	+++	98
8	61	m	IgG	28	0	23	II	0	MM	+++	100
9	62	m	IgG	69	>10	30	II	0	MM	++	100
10	62	f	IgG	70	>10	80	III	1	MM	+	95
11	68	m	IgA	36	>10	60	I	0	MM	+++	100
12	69	m	–	–	3	50	I	1	nsMM	+++/+	95
13	71	m	IgG	26	0	30	I	0	MM	+++	100
14	72	m	IgG	13	0	29	I	0	MM	+++	100
15	74	m	IgG	20	0	23	I	0	MM	+++	100
16	75	m	IgA	40	0	78	II	0	MM	++	88
17	77	m	IgG	45	0	34	II	0	MM	+++	100
18	79	f	IgG	23	0	16	I	0	MM	+++	100
19:1	79	m	IgG	24	7	50	III	0	MM	+++	93
19:2	79	m	IgG	3	n/a	n/a	–	1	MM	+++	95
19:3	80	m	IgG	3	n/a	16	–	2	MM	+++	91
20	82	m	IgA	29	0	44	III	0	MM	+++	100
21	83	f	IgG	39	0	89	III	0	MM	+++	93
22	84	m	IgA	17	0	38	III	0	MM	+++	86
23	61	m	IgA	7	2	24	–	0	AL	++	97
24	64	f	–	–	n/a	6	–	0	AL	+++	100
25	72	f	–	–	0	1	–	0	LCDD/MM	+++	98
26	61	f	IgA	42	n/a	80	–	4	PCL	+++	76
27	75	m	IgG	18	>10	8	–	4	PCL	+	77
28	52	m	IgG	1	1	5	–	1	PC	+++	93
29	60	f	IgG	4	1	2	–	1	PC	+++	100

n/a, not analyzed.
[a]Corresponds to number found in Figure 3.
[b]m, male; f, female.
[c]Immunoglobulin class of M-component.
[d]Number of skeletal destructions.
[e]Multiple myeloma cells counted as percent of all nucleated cells in bone marrow smears.
[f]International Staging System of MM.
[g]Number of different MM treatment regimens before BI-505 analysis.
[h]MM, multiple myeloma; nsMM, nonsecretory multiple myeloma; AL, amyloid light-chain amyloidosis; LCDD, light-chain deposit disease; PCL, plasma cell leukemia; PC, plasmacytoma.
[i]Measured by FACS on MM cells. Two patients (no. 3 and 12) had two MM cell populations with differential BI-505 expression.

BI-505-treated mice were not significantly different from mice treated with BI-505 only ($V_{BI\text{-}505}$ = 95 ± 39 mm^3, $V_{BI\text{-}505+asialo}$ = 130 ± 53 mm^3, $p > 0.05$) but were significantly smaller compared to control-antibody-treated animals ($p < 0.01$, Figure 6E). BI-505 also had significant antitumor activity in two different aggressively growing NK-cell-deficient MM mouse models comprising RPMI-8226 or U266 cells grafted to NOD/Shi-*scid*/*IL-2Rγ*$^{-/-}$ mice (Figures 6F and 6G). Taken together, our data identify macrophages, but not NK cells, as critical effector cells conferring BI-505 FcγR-dependent in vivo antitumor activity.

We next investigated BI-505's ability to mediate Fc:FcγR-dependent macrophage phagocytosis (antibody-dependent cell phagocytosis [ADCP]) of human MM cells in vitro. As expected, BI-505 IgG_1 bound to human FcγR (Figure 6C) and

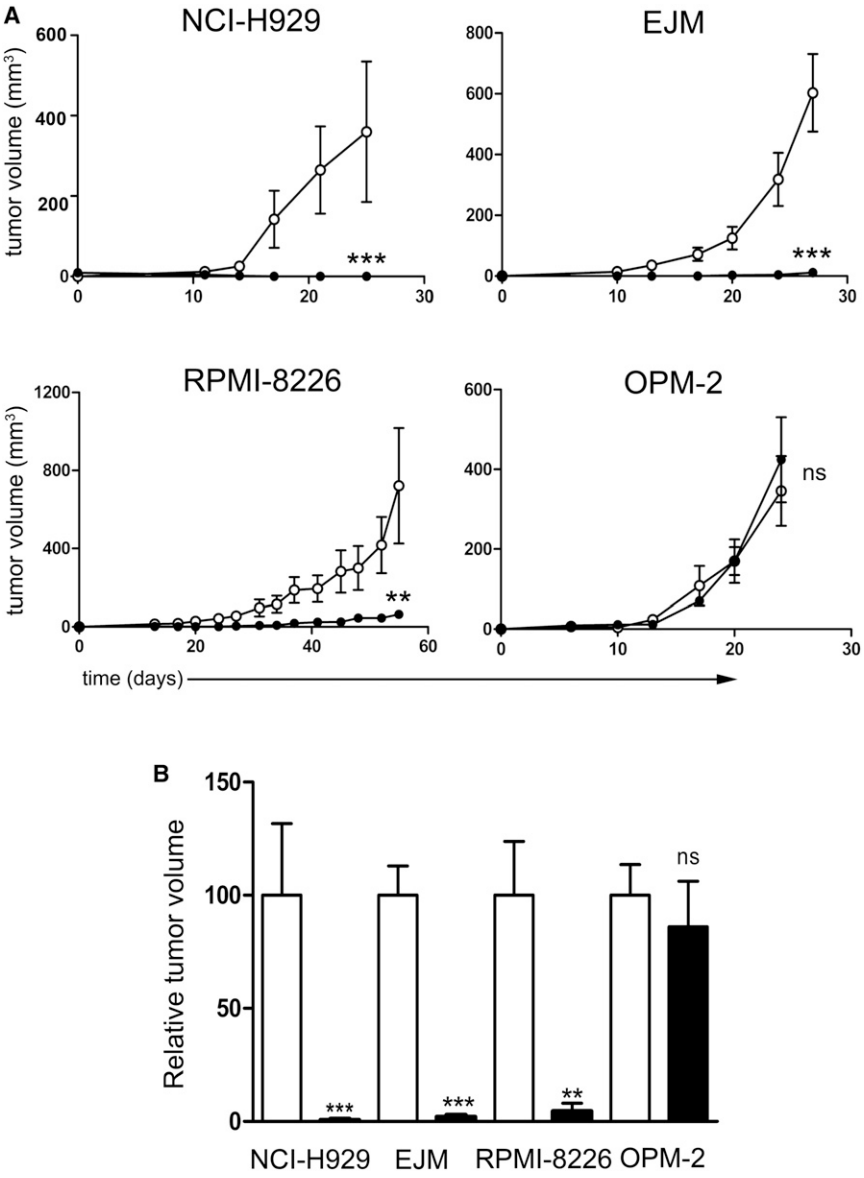

Figure 4. BI-505 Has Broad and ICAM-1-Dependent Anti-MM Activity In Vivo

(A) Tumor volume (mean ± SD) of NCI-H929 (ICAM-1$^+$), EJM (ICAM-1$^+$), RPMI-8226 (ICAM-1$^+$), and OPM-2 (ICAM-1$^-$) MM models after treatment with 2 mg/kg BI-505 (filled circles) or control (open circles) antibody.

(B) Relative tumor volumes following treatment with 2 mg/kg BI-505 (filled bars) or control (open bars) antibody in NCI-H929, EJM, RPMI-8226, and OPM-2 MM models. Graph shows tumor volumes (mean ± SD) relative to the mean tumor volume of control IgG-treated animals. There were eight animals per treatment group.

**p < 0.01, ***p < 0.001; ns, not statistically different.

conferred ADCP of both RPMI-8226 and primary patient's MM cells (Figures 6H and 6I) in the presence of human macrophages. In contrast, FcγR-binding-deficient BI-505 IgG1$_{N297Q}$ did not bind to human FcγR (Figure 6C) and did not confer ADCP of targeted MM cells (Figures 6H–6J). Similarly, preincubation with recombinant-soluble Fc gamma receptor diminished BI-505 IgG$_1$-mediated ADCP (Figure 6J). Therefore, analogous to the in vivo setting, BI-505-mediated ADCP in vitro was Fc: Fc gamma receptor dependent.

We also examined the ability of BI-505 to mediate antibody-dependent cell cytotoxicity (ADCC) against human target tumor cells in the presence of human effector NK cells. BI-505 conferred cytotoxicity in an Fc-dependent manner, although ADCC activity by effector NK cells was less pronounced compared with macrophage-mediated ADCP (data not shown).

Besides Fc:FcγR-dependent antitumor mechanisms, cancer mAb Fc-dependent antitumor activity may result from activation of the complement cascade by complement-dependent cytotoxicity (CDC). We therefore examined the ability of BI-505 to induce CDC in a panel of ICAM-1-expressing tumor cell lines. However, BI-505 did not induce CDC in any of the tumor cell lines monitored (data not shown). In contrast, treatment with the positive control rituximab effectively induced CDC, as has previously been reported (Cragg and Glennie, 2004; Cragg et al., 2003; Manches et al., 2003).

In summary, our data provide strong evidence for Fc:FcgR-dependent antitumor mechanisms, e.g., macrophage-mediated ADCP and FcγR cross-linking-induced antibody tumor PCD underlying BI-505's therapeutic activity.

Safety Profile of the BI-505 Antibody

In addition to exerting significant antitumor activity, a therapeutic cancer antibody must be safe and tolerable for patients. Toxicology studies in relevant animal species may provide important information on drug safety. BI-505 does not, however, cross-react with ICAM-1 from animals that are commonly used for toxicological evaluation (data not shown). Our nonclinical safety assessment therefore focused on evaluating its effects on viability and function of human normal (untransformed) cells expressing ICAM-1.

Based on BI-505's documented ability to confer Fc:FcγR-dependent antitumor activity in malignant B cells, and a proposed general negative role for complement activation with regard to antibody tolerability (Lim et al., 2010; van der Kolk et al., 2001), we examined direct cytotoxic effects (PCD, ADCC, and CDC) of BI-505 in ICAM-1-expressing human peripheral blood B cells and endothelial cells. Whereas peripheral blood B cells and naive B cells show low endogenous expression of the BI-505 epitope (Fransson et al., 2006), human umbilical vascular endothelial cells (HUVECs) and human microvascular endothelial cells (HMVECs) cells showed significant ICAM-1

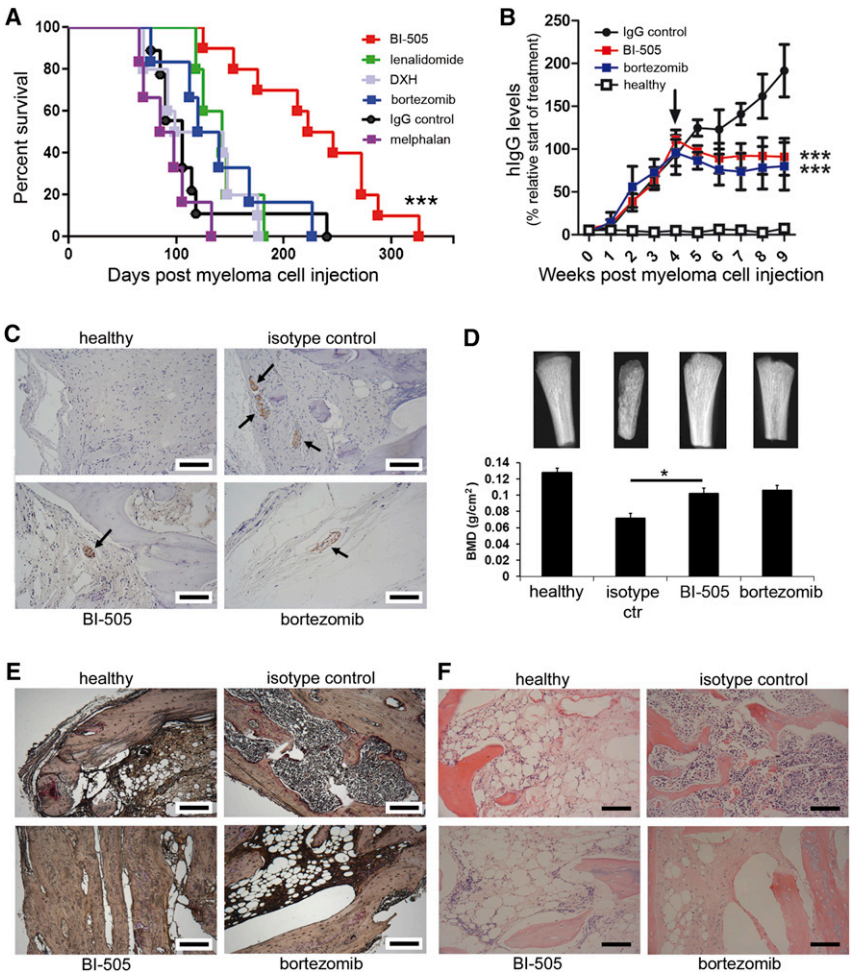

Figure 5. BI-505 Confers Enhanced Survival Compared to Currently Used Treatments in Disseminated Experimental Models of Advanced MM

(A) Animal survival in advanced disseminated RPMI-8226 myeloma model following treatment with control antibody, lenalidomide, bortezomib, dexamethasone (DXH), melphalan, or BI-505. ***$p < 0.001$.

(B) Human immunoglobulin G (hIgG) (mean ± SD) in SCID-hu mice after myeloma cell inoculation and drug treatment. Graph shows pooled data from two independent experiments, each with MM cells obtained from two different patient donors (n = 4). The percentage of hIgG levels compared to start of treatment (arrow) was monitored. ***$p < 0.001$.

(C) Myeloma tumor burden in implanted bones harvested from drug-treated mice. Pictures show representative images of tumor burden as assessed by immunohistochemistry following staining for human CD138-expressing cells. Arrows indicate human CD138-positive myeloma cell regions. Scale bar = 50 μm.

(D) X-radiographic quantification of bone mineral density. Radiographs of implanted human bones receiving drug or control treatment were harvested from mice at end of experimentation (10 weeks postmyeloma cell injection and following 6 weeks of drug treatment). Upper panel shows representative radiographs of bones from healthy mice, control IgG-treated mice, BI-505-treated mice, or bortezomib-treated mice (left to right). Lower panel shows mean ± SD bone mineral density of mice receiving treatment as indicated. *$p < 0.05$.

(E and F) Representative images of trap staining (purple stain) for detection of osteoclasts (E) or hematoxylin and eosin staining for detection of infiltrated nucleated cells (F) performed on healthy and MM cell-injected bones harvested from SCID-hu mice treated as indicated at end of experimentation. Scale bar = 100 μm.

See also Figure S3.

expression, which was further upregulated in response to IFN-γ stimulation as determined by flow cytometric analyses (Figure S5). However, BI-505 did not induce cell death in any of the resting or activated normal ICAM-1-expressing cell types that were examined, regardless of whether or not antibody was crosslinked to mimick Fc:FcγR-crosslinking in vivo (Figures 7A–7C and 7G). In contrast, treatment of endothelial cells with paclitaxel and treatment of B cells with positive control anti-HLA-DR or anti-CD20 antibody induced significant PCD (Figures 7A and 7G).

Cytokine release and T cell proliferation are thought to be common causes of mild and severe adverse reactions to antibody therapy. In order to further investigate any undesirable effects of BI-505 on ICAM-1-expressing immune cells, we therefore assessed putative effects of BI-505 on peripheral blood mononuclear cells (PBMCs) cytokine release and T cell proliferation. In order to maximize the chances of identifying any PBMC-agonistic properties of BI-505, we used two different antibody-coating protocols in which the antibody was hypercrosslinked as previously described (Stebbings et al., 2007). BI-505 immobilized by either protocol induced PCD in Daudi lymphoma cells, demonstrating that biological activity was retained following immobilization (data not shown). BI-505 did not, however, induce PBMC cytokine release and did not induce T cell proliferation by either immobilization protocol or when added in solution in the presence or absence of crosslinking reagent (Figures 7D–7F). In contrast and as expected, incubation of PBMCs with an immobilized positive control anti-CD3 antibody resulted in significant release of IL-1β, IL-2, IL-6, IL-8, TNF-α, and IFN-γ (Figure 7D). Analogous experiments demonstrated that BI-505 added in solution did not induce or enhance cytokine release from resting or lipopolysaccharide prestimulated PBMCs and did not induce T cell proliferation (Figures 7E and 7F).

Taken together therefore, we have found no evidence for undesirable activation or cytotoxicity of BI-505 against ICAM-1-expressing immune cells. Together with limited safety studies in rat, rabbit, and monkey, demonstrating no compound-related off-target toxicity (data not shown), and indicating a long half-life typical of that for a human IgG (i.e., 12–13 days in rat [Table S2], corresponding to 2–3 weeks in man), these observations indicated a therapeutically relevant safety profile and pharmacokinetics of BI-505.

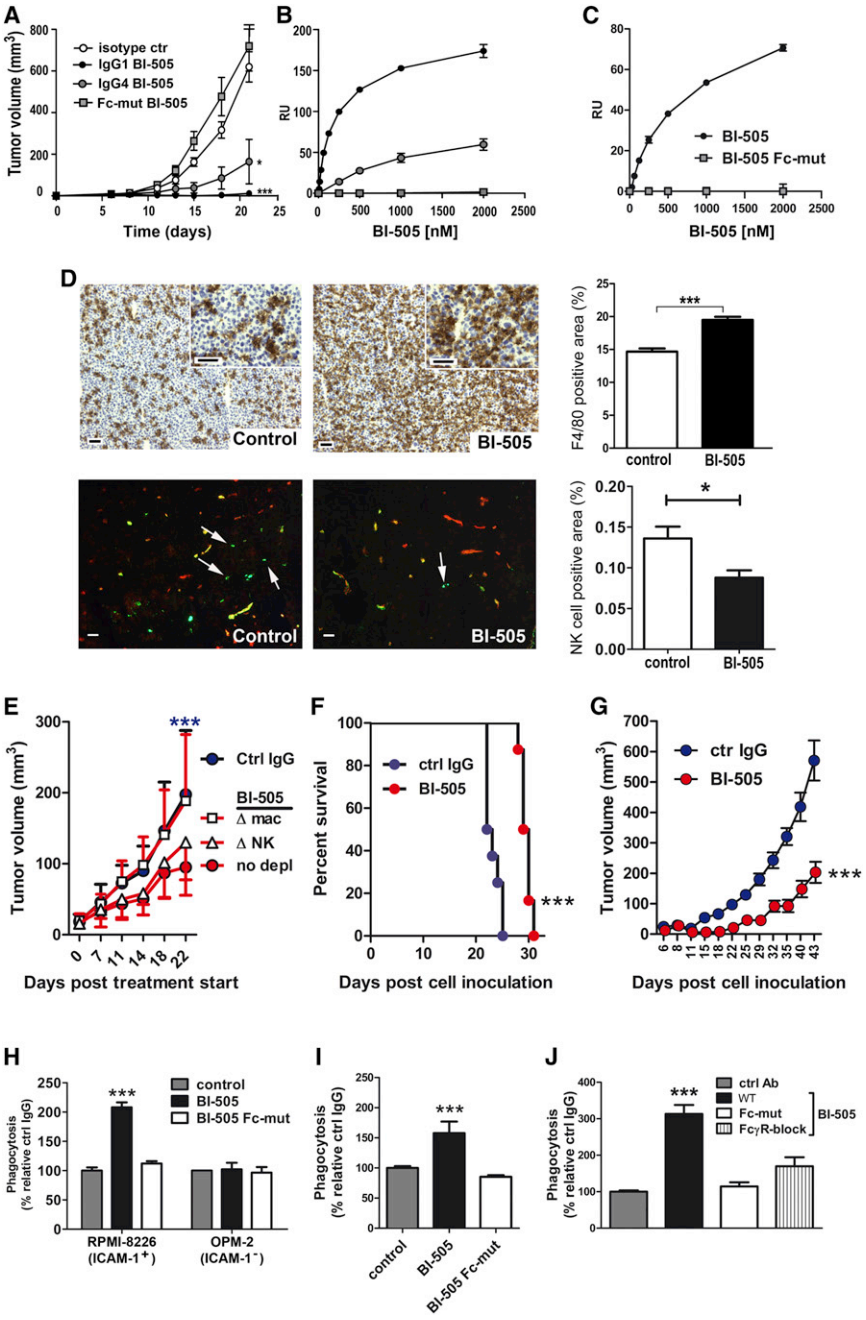

Figure 6. BI-505 Confers Fc-FcγR-Dependent Antitumor Activity through Macrophages

(A) Mean tumor volume of SCID mice bearing established ARH-77 tumors and treated with isotype control antibody or BI-505 IgG_1, BI-505 IgG_4, or BI-505 $IgG_{1\ N297Q}$ (Fc-variant) antibodies. $^*p < 0.05$, $^{**}p < 0.01$.

(B) BiaCore analysis of BI-505 Fc-variant antibodies binding to mouse FcγRIV.

(C) BiaCore analysis of BI-505 Fc-variant antibodies binding to human FcγRIIIa.

(D) Immunohistochemical quantitation of F4/80$^+$ macrophages (top panel) or NK cells (lower panel) in tumor tissue of animals bearing established ARH-77 tumors treated with control antibody or BI-505. Graphs show mean F4/80$^+$ and NK-cell-positive tumor areas, respectively. Bar = 40 μm. $^*p < 0.05$, $^{***}p < 0.001$.

(E) Tumor growth in macrophage or NK-cell-depleted SCID mice bearing established RPMI-8226 myeloma tumors treated with BI-505 or control antibody. $^{***}p < 0.001$.

(F) Animal survival following BI-505 or control antibody treatment in a disseminated NK-cell-deficient NOD/Shi-*scid*/*IL-2Rγ*$^{-/-}$ mouse model comprising i.v. grafted U266 myeloma cells. $^{***}p < 0.001$.

(G) Tumor growth in BI-505 or control antibody-treated NK-cell-deficient NOD/Shi-*scid*/*IL-2Rγ*$^{-/-}$ mice transplanted with RPMI-8226 myeloma cells. $^{***}p < 0.001$.

(H) Macrophage ADCP of RPMI-8226 and OPM-2 myeloma cells. n = 4, $^{***}p < 0.001$.

(I) Macrophage-mediated ADCP of primary multiple myeloma cells. n = 2, $^{***}p < 0.001$.

(J) Macrophage ADCP of ICAM-1$^+$ EJM myeloma cells. n = 2, $^{***}p < 0.001$.

There were eight to ten animals per treatment group. Error bars show ± SD.

See also Figure S4 and Table S1.

DISCUSSION

We report the successful application of a function-first approach to therapeutic antibody discovery, resulting in the isolation of a human ICAM-1 antibody based on its (1) specificity for a surface receptor upregulated on tumor B cells, (2) significant tumor programmed-cell-death-inducing properties, and (3) significant in vivo antitumor activity against human B cell tumors. Thus, our functional screening methodology was successfully applied both to identify a function (induction of PCD in tumor cells) of a well-characterized receptor (ICAM-1) and a human antibody against the same target with significant therapeutic potential.

Our function-first approach to antibody discovery offers several advantages over and differs in several respects from conventional approaches in which antibodies are identified based on specificity for a predefined target structure. By combining powerful differential biopanning of a naive human antibody library with high-throughput tumor cell death screening, our discovery platform enables the simultaneous generation of multiple high-affinity antibodies with therapeutic potential and specificity for different tumor-cell-associated receptors. The value of screening for functionality across different specificities has been indicated by previous studies, which collectively demonstrate that antibodies against different tumor-associated cell surface receptors can have significant antitumor activity against the same cancer cell type (for a review, see Cheson and Leonard [2008]). Thus, in a highly diversified antibody source, such as n-CoDeR, the most therapeutically efficacious, potent, and best-tolerated antibodies with respect to a given type of cancer

could be specific for one of several receptors, and identifying the optimal antibodies requires functional screening of antibodies targeting all such receptors.

The predictive value of tumor PCD as an indicator of an antibody's therapeutic potential was demonstrated by the enhanced in vivo antitumor activity of BI-505 against CD20-expressing tumors, compared to rituximab. Cragg and Glennie (2004) further indicate the importance of using a function-first approach and of screening for tumor PCD. Different antibodies, which bound with similar affinity to CD20 and had identical Fc regions, differed greatly in their therapeutic efficacy in vivo and, intriguingly, conferred antitumor activity by different mechanisms of action. Superior therapeutic activity correlated positively with tumor PCD and inversely with complement-dependent tumor cell cytotoxicity (Beers et al., 2008; Cragg and Glennie, 2004). These and other observations highlight the importance of the function-first approach to identify antibodies with therapeutic activity (Beck et al., 2010; Gan et al., 2009; Ivanov et al., 2009). Our use of cancer cells, which expressly targeted antigens in their true cell surface configuration, should increase the likelihood of identifying antibodies with specificity for functional and disease-associated receptor epitopes compared to conventional techniques using recombinant antigen or transfected cells in the panning process. Finally, it is generally thought that therapeutic targets are limited and that most might already be identified. From this perspective, it is noteworthy that our technology can reveal functions of previously well-characterized receptors, indicating their suitability as targets in previously unrecognized indications and expand the "therapeutic target space." Thus, whereas the well-characterized role of ICAM-1 in inflammation has provided the rationale for anti-ICAM-1 targeted intervention of acute and chronic inflammatory disorders (Kavanaugh et al., 1997; Mileski et al., 2003; Schneider et al., 1998), our findings identify ICAM-1 as a promising target in multiple MM and possibly oncology in a broader sense. Taken together, our function-first approach provides an effective strategy to generate antitumor antibodies, such as BI-505.

Several observations suggest that ICAM-1 may be a suitable target for MM immunotherapy. Strong expression of ICAM-1 is associated with advanced disease, poor survival, and resistance to chemotherapy (Sampaio et al., 2009; Schmidmaier et al., 2006; Zheng et al., 2012), which is the current inevitable end-stage of MM (Kyle and Rajkumar, 2004). Consistent with these observations, we demonstrate that a majority of MM cells express high levels of the epitope targeted by BI-505. High and homogenous expression on the tumor cell surface and upregulated expression in conjunction with disease progression and the development of resistance to chemotherapy are hallmarks of targets suitable for therapy with antibodies that confer direct tumor cell cytotoxicity. The antitumor activity of BI-505 correlated with antibody binding to tumor-cell-expressed ICAM-1 and was shown to be Fc:FcγR dependent. Accumulating evidence suggests that interactions between an antibody's constant domain (Fc) and a host's Fc gamma receptors (FcγR) are instrumental in the therapeutic efficacy of rituximab and other approved anticancer antibodies (Bibeau et al., 2009; Lejeune et al., 2008; Musolino et al., 2008; Weng and Levy, 2003; Zhang et al., 2007) via mechanisms that may involve both innate and adaptive immunity (Alduaij and Illidge, 2011; Park et al., 2010), as well as enhanced tumor PCD following FcγR-dependent crosslinking of tumor bound mAb (Wilson et al., 2011). Consequently, although there is currently no antibody available to treat MM, nonclinical and clinical studies on antibodies approved for treatment of different types of cancer suggest that those—like BI-505—that are capable of triggering MM cell death via Fc:FcγR-dependent immunity hold particular promise of improving MM survival. Our finding that macrophages are principal effector cells conferring BI-505 FcγR-dependent antitumor activity is intriguing. Macrophages are abundantly present in MM bone marrow and accumulating data point to a detrimental role for macrophages and ICAM-1 in MM development of drug resistance (Zheng et al., 2009, 2012). BI-505 harnessing of tumor-associated macrophages to confer antitumor activity thus appears an attractive mechanism of combatting MM.

In addition to exerting significant antitumor activity, a therapeutic cancer antibody must be safe and tolerable for patients. Previous studies by independent investigators demonstrated that treatment with (a murine) anti-ICAM-1 antibody was well tolerated by different patient groups (Kavanaugh et al., 1997; Mileski et al., 2003; Schneider et al., 1998). Herein presented data on BI-505 is consistent with this notion. Owing to its fully human nature, and as indicated from our animal studies, BI-505 should have low immunogenicity.

Collectively, our results demonstrate proof-of-principle for the function-first approach in the search for efficient antitumor antibodies and provide a rationale for further preclinical and clinical evaluation of BI-505 in the treatment of MM. An open-label multicenter phase I dose-escalation study with BI-505 in relapsed/refractory MM patients, approved by the Swedish Medical Product Agency and in accordance with the United States Food and Drug Administration's (FDA) guidance, is ongoing (NCT01025206; http://clinicaltrials.gov/).

EXPERIMENTAL PROCEDURES

Cell Culture and In Vitro Assays

ARH-77, RPMI-8226, and Daudi cell lines were obtained from the American Type Culture Collection (ATCC, Sweden). NCI-H929, EJM, and OPM-2 cell lines were obtained from the Deutsche Sammlung von Mikroorganismen und Zellkulturen (DSMZ, Germany). HUVEC and HMVEC cells were obtained from Cascade Biologics (Portland, OR, USA). Cells were maintained in culture media as recommended by the supplier and maintained at 37°C in a 5% CO_2, 95% humidity incubator. Cell PCD, ADCC, CDC, cytokine release, and T cell proliferation assays were performed as described elsewhere (Fransson et al., 2006; Supplemental Experimental Procedures).

Patient Cell Studies

Plasma cell surface expression of ICAM-1 and the BI-505 epitope was analyzed by fluorescence-activated cell sorting (FACS). Bone marrow aspirates were obtained from 29 patients diagnosed with MM or related diseases at the Department of Hematology, Skånes University Hospital, Lund. All human samples were collected using protocols approved by the Ethics Committee of Skåne University Hospital, and informed consent was obtained from all patients.

Animal Studies

Studies were conducted in accordance with guidelines of the Lund University Hospital, Sweden, or University of Utah, Salt Lake City, USA, following approval from the local ethical committee for animal care and use. BI-505 efficacy and potency was examined in subcutaneous and disseminated, prophylactic and therapeutic, experimental MM models comprising myeloma cell lines RPMI-8226, U266, EJM, and OPM-2. The in vivo efficacy of BI-505 was compared to clinically approved drugs dexamethasone, melphalan,

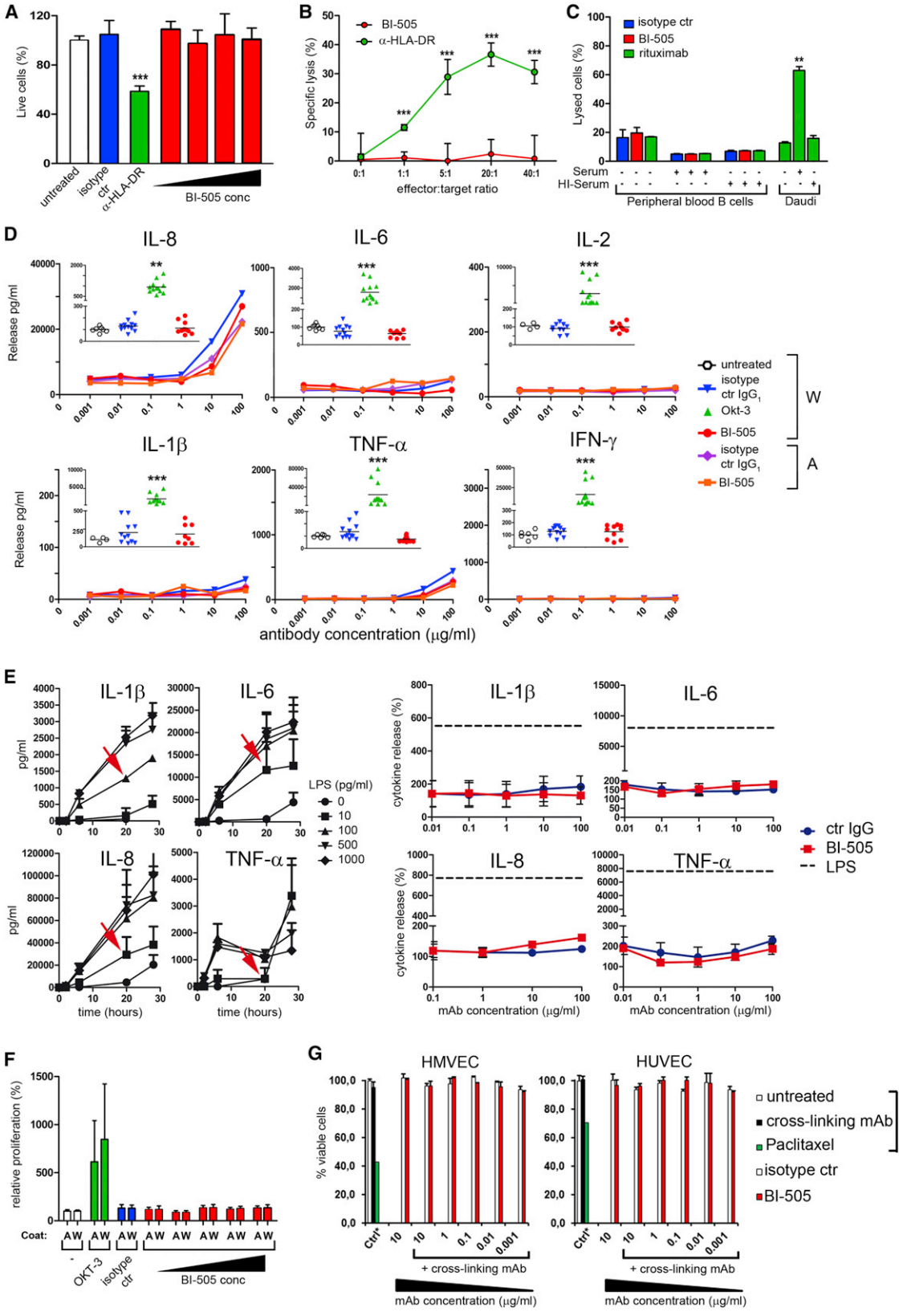

(legend on next page)

bortezomib, and revlimid used at clinically relevant doses in therapeutic disseminated models comprising RPMI-8226 or primary patient myeloma cells, the latter following injection of patient cells in implanted of human fetal bone in SCID mice. For subcutaneous grafting, 1–5 × 10^6 tumor cells (RPMI-8226, NCI-H929, EJM, OPM-2, ARH-77, or Daudi) were subcutaneously injected at a volume of 100 μl into the left flank of anesthetized mice as described in the Supplemental Experimental Procedures. For established xenograft studies, when tumors reached an average size of 80–120 mm^3, animals were sorted to give nearly identical group mean tumor sizes and were treated with isotype control antibody (20 mg/kg/inj), rituximab (20 mg/kg/inj), or BI-505 antibody (0.02 to 20 mg/kg/inj, as indicated in the text) intraperitoneally (i.p.) twice weekly until study termination. For disseminated experimental models of MM, RPMI-8226 (10 × 10^7 tumor cells) were injected intravenously (i.v.) into the caudal vein of anesthetized mice after whole-body irradiation (1.8 Gy, ^{60}Co, INRA, Bretennieres). Treatment with saline, isotype control IgG, bortezomib, lenalidomide, dexamethasone, or BI-505 started on day 5 (RPMI-8226). Treatment with melphalan started on day 10. BI-505 or isotype IgG mAb was administered i.v. at 2 mg/kg/inj twice weekly for 8 weeks; bortezomib at 1 mg/kg/inj once weekly for 8 weeks; lenalidomide orally at 2 mg/kg/inj for two cycles consisting of 5 days of treatment and 2 days of wash out; melphalan i.v. at 3 mg/kg/inj once weekly for 8 weeks; and dexamethasone at 6 mg/kg/inj three times weekly for 2 weeks. In vivo mechanistic studies assessing the role of Fc-FcγR interactions utilized wild-type and engineered FcγR-binding-deficient (N297Q) IgG1 variants of BI-505. The role of macrophages and NK cells for BI-505 in vivo antitumor activity was assessed using anti-asialo antibody treatment, clodronate liposome treatment, or NK-cell-deficient mice. For a detailed description of in vivo studies, see the Supplemental Experimental Procedures.

In Vitro Functional Studies

Peripheral blood-derived monocytes, NK cells, B cells, and T cells were purified from buffy coats from healthy donors obtained from the local blood central at Lund University Hospital and Halmstad Hospital. Briefly, PBMCs were first extracted using Ficoll-Paque PLUS (GE Healthcare Life Sciences, Waukesha, WI, USA), followed by isolation of monocytes with CD14 MicroBeads and MACS Separation (Miltenyi Biotec, Bergisch Gladbach, Germany). Monocyte-derived macrophages were generated by 6–14 days culture in the presence of 25 ng/ml of recombinant human M-CSF (R&D Systems, Minneapolis, MN, USA). For multiple myeloma cells, freshly isolated bone marrow samples were donated by patients at Lund University Hospital and subsequently processed with Ficoll-Paque PLUS. Negative isolation of malignant plasma cells was performed using Plasma Cell Isolation Kit II (Miltenyi Biotec).

ADCP

Cultured macrophages were detached and plated in flat 96-well plates at 50,000 cells/well and placed in 37°C. Carboxyfluorescein succinimidyl ester (CFSE)-stained target cells were incubated with antibodies for up to 1 hr on ice. After washing, the different cell solutions were added to the culture plates containing macrophages at a ratio of 5:1 (target cells:macrophages). Thereafter, the culture plates were incubated at 37°C for 1–2 hr (primary patient MM cells) or 16 hr (RPMI-8226 cells). The percentage of macrophages that had phagocytosed tumor cells ($CFSE^+$, $CD206^+$) per total analyzed macrophages was determined following gating and acquisition of 5,000 $CD206^+$ cells/sample.

ADCC

NK cells were isolated from purified PBMCs using positive or negative NK cell isolation kits (Miltenyi Biotec). Target cells were harvested and incubated in medium with or without the respective antibodies (2 μg/ml) for 60 min on ice before. NK cells were washed, diluted in ADCC medium, and dispensed together with the respective antibody-coated target cells at varying effector/target cell ratios. Experiments were performed in triplicate. After incubation, TO-PRO-3 dye and counting beads (Invitrogen, Carlsbad, CA, USA) were added, and cells were analyzed for membrane permeabilization using flow cytometry.

CDC

Target cells were harvested as described above (under the ADCC heading) and incubated with antibodies at 5 μg/ml for 60 min on ice and then washed. Human serum, normal or heat-inactivated (Sigma, Sweden), was added to tubes, and the samples were incubated for 2 hr at 37°C. After completion of incubation, ToPo-Pro-3 (Invitrogen) was added at a final concentration of 0.3 μM, and cells were analyzed for membrane permeabilization using flow cytometry.

Detailed Experimental Procedures, including protocols for assessment of apoptosis in normal ICAM-1-expressing endothelial cell, T cell proliferation, PBMC cytokine release, and receptor occupancy studies, are described in the Supplemental Experimental Procedures.

SUPPLEMENTAL INFORMATION

Supplemental Information includes five figures, two tables, and Supplemental Experimental Procedures and can be found with this article online at http://dx.doi.org/10.1016/j.ccr.2013.02.026.

ACKNOWLEDGMENTS

We thank Professor Tor Olofsson for help with FACS analyses and Professors Mark Cragg and Christer Betsholtz for critically reviewing our manuscript. M.H. was supported by a grant from The Royal Swedish Academy of Sciences. N.V., A.S., A.L., L.D., Z.C.L., T.M.-N., T.L., M.K., A.L., L.M., and B.F. are or were employees of BioInvent International during their contribution to this paper.

Figure 7. BI-505 Does Not Induce Apoptosis, ADCC, CDC, T Cell Proliferation, or Cytokine Release in Resting or Stimulated Normal Cells Expressing ICAM-1

(A) Apoptosis in peripheral blood B cells. Graph shows percent live (nonapoptotic) B cells following no treatment or treatment with isotype control IgG, anti-HLA-DR (positive control IgG), or BI-505 (0, 1.5, 6, or 24 μg/ml). Values were normalized to untreated cells, where percent living cells was set to 100.

(B) ADCC of peripheral blood B cells. Graph shows specific lysis of target peripheral blood B cells following treatment with BI-505 or anti-HLA-DR IgG_1 (positive control). Values were normalized to treatment with isotype control IgG, where specific lysis was set to 0%.

(C) CDC of peripheral blood B cells and Daudi Burkitt's lymphoma cells. Cells were incubated with BI-505, rituximab, or isotype control IgG and analyzed for CDC.

(D) Antibody-induced PBMC cytokine release. PBMC cytokine release was measured by ELISA of cell culture supernatants for IL-1β, IL-2, IL-6, IL-8, IFN-γ, and TNF-α following incubation of cells in plates coated with hypercrosslinked (air-dried "A" or wet-coated "W") BI-505, isotype control, or positive-control Okt-3 antibody.

(E) Antibody-induced cytokine release in lipopolysaccharide (LPS)-primed PBMCs. PBMCs were incubated with titrated LPS, and concentrations yielding submaximal cellular release of IL-1β (100 pg/ml), IL-6 (10 pg/ml), IL-8 (10 pg/ml), and TNF-α (10 pg/ml) were determined (arrows, left panel) and used in subsequent experiments assessing antibody (BI-505 or control IgG) effects on cytokine release from LPS-primed PBMCs (right panel). Treatment with 100 ng/ml LPS served as positive control for robust cytokine release.

(F) Antibody-induced T cell proliferation. CFSE-labeled T cells were incubated with BI-505, isotype control IgG, or anti-CD3 (okt-3) IgG hyperimmobilized to cell culture plates by air-drying "A" or wet-coating "W." Cells were cultured for 6 days, and T cell proliferation was monitored by flow cytometry as decreased CFSE signals.

(G) Antibody-induced endothelial cell apoptosis. HUVEC or HMVEC endothelial cells were incubated with paclitaxel (positive control), BI-505, or isotype control IgG in the presence or absence of crosslinking mAb. Apoptosis was measured by flow cytometry following staining of cells with annexin V-AF488.

**$p < 0.01$, ***$p < 0.001$. Error bars show ± SD.

See also Figure S5; Table S2.

Received: September 14, 2010
Revised: August 29, 2012
Accepted: February 27, 2013
Published: April 15, 2013

REFERENCES

Aalinkeel, R., Nair, M.P.N., Sufrin, G., Mahajan, S.D., Chadha, K.C., Chawda, R.P., and Schwartz, S.A. (2004). Gene expression of angiogenic factors correlates with metastatic potential of prostate cancer cells. Cancer Res. *64*, 5311–5321.

Alduaij, W., and Illidge, T.M. (2011). The future of anti-CD20 monoclonal antibodies: are we making progress? Blood *117*, 2993–3001.

Beck, A., Wurch, T., Bailly, C., and Corvaia, N. (2010). Strategies and challenges for the next generation of therapeutic antibodies. Nat. Rev. Immunol. *10*, 345–352.

Beers, S.A., Chan, C.H., James, S., French, R.R., Attfield, K.E., Brennan, C.M., Ahuja, A., Shlomchik, M.J., Cragg, M.S., and Glennie, M.J. (2008). Type II (tositumomab) anti-CD20 monoclonal antibody out performs type I (rituximab-like) reagents in B-cell depletion regardless of complement activation. Blood *112*, 4170–4177.

Bibeau, F., Lopez-Crapez, E., Di Fiore, F., Thezenas, S., Ychou, M., Blanchard, F., Lamy, A., Penault-Llorca, F., Frébourg, T., Michel, P., et al. (2009). Impact of FcgammaRIIa-FcgammaRIIIa polymorphisms and KRAS mutations on the clinical outcome of patients with metastatic colorectal cancer treated with cetuximab plus irinotecan. J. Clin. Oncol. *27*, 1122–1129.

Cheson, B.D., and Leonard, J.P. (2008). Monoclonal antibody therapy for B-cell non-Hodgkin's lymphoma. N. Engl. J. Med. *359*, 613–626.

Clynes, R.A., Towers, T.L., Presta, L.G., and Ravetch, J.V. (2000). Inhibitory Fc receptors modulate in vivo cytotoxicity against tumor targets. Nat. Med. *6*, 443–446.

Cragg, M.S., and Glennie, M.J. (2004). Antibody specificity controls in vivo effector mechanisms of anti-CD20 reagents. Blood *103*, 2738–2743.

Cragg, M.S., Morgan, S.M., Chan, H.T., Morgan, B.P., Filatov, A.V., Johnson, P.W., French, R.R., and Glennie, M.J. (2003). Complement-mediated lysis by anti-CD20 mAb correlates with segregation into lipid rafts. Blood *101*, 1045–1052.

Fransson, J., Tornberg, U.C., Borrebaeck, C.A., Carlsson, R., and Frendéus, B. (2006). Rapid induction of apoptosis in B-cell lymphoma by functionally isolated human antibodies. Int. J. Cancer *119*, 349–358.

Gan, H.K., Lappas, M., Cao, D.X., Cvrljevdic, A., Scott, A.M., and Johns, T.G. (2009). Targeting a unique EGFR epitope with monoclonal antibody 806 activates NF-kappaB and initiates tumour vascular normalization. J. Cell. Mol. Med. *13* (9B), 3993–4001.

Hideshima, T., Mitsiades, C., Tonon, G., Richardson, P.G., and Anderson, K.C. (2007). Understanding multiple myeloma pathogenesis in the bone marrow to identify new therapeutic targets. Nat. Rev. Cancer *7*, 585–598.

Huang, Y.W., Richardson, J.A., and Vitetta, E.S. (1995). Anti-CD54 (ICAM-1) has antitumor activity in SCID mice with human myeloma cells. Cancer Res. *55*, 610–616.

Ivanov, A., Beers, S.A., Walshe, C.A., Honeychurch, J., Alduaij, W., Cox, K.L., Potter, K.N., Murray, S., Chan, C.H., Klymenko, T., et al. (2009). Monoclonal antibodies directed to CD20 and HLA-DR can elicit homotypic adhesion followed by lysosome-mediated cell death in human lymphoma and leukemia cells. J. Clin. Invest. *119*, 2143–2159.

Johnson, J.P., Stade, B.G., Hupke, U., Holzmann, B., and Riethmüller, G. (1988). The melanoma progression-associated antigen P3.58 is identical to the intercellular adhesion molecule, ICAM-1. Immunobiology *178*, 275–284.

Kapoor, P., Greipp, P.T., Morice, W.G., Rajkumar, S.V., Witzig, T.E., and Greipp, P.R. (2008). Anti-CD20 monoclonal antibody therapy in multiple myeloma. Br. J. Haematol. *141*, 135–148.

Kavanaugh, A.F., Schulze-Koops, H., Davis, L.S., and Lipsky, P.E. (1997). Repeat treatment of rheumatoid arthritis patients with a murine anti-intercellular adhesion molecule 1 monoclonal antibody. Arthritis Rheum. *40*, 849–853.

Kyle, R.A., and Rajkumar, S.V. (2004). Multiple myeloma. N. Engl. J. Med. *351*, 1860–1873.

Lejeune, J., Thibault, G., Ternant, D., Cartron, G., Watier, H., and Ohresser, M. (2008). Evidence for linkage disequilibrium between Fcgamma RIIIa-V158F and Fcgamma RIIa-H131R polymorphisms in white patients, and for an Fcgamma RIIIa-restricted influence on the response to therapeutic antibodies. J. Clin. Oncol. *26*, 5489–5491, author reply 5491–5492.

Lim, S.H., Beers, S.A., French, R.R., Johnson, P.W., Glennie, M.J., and Cragg, M.S. (2010). Anti-CD20 monoclonal antibodies: historical and future perspectives. Haematologica *95*, 135–143.

Manches, O., Lui, G., Chaperot, L., Gressin, R., Molens, J.P., Jacob, M.C., Sotto, J.J., Leroux, D., Bensa, J.C., and Plumas, J. (2003). In vitro mechanisms of action of rituximab on primary non-Hodgkin lymphomas. Blood *101*, 949–954.

Mileski, W.J., Burkhart, D., Hunt, J.L., Kagan, R.J., Saffle, J.R., Herndon, D.N., Heimbach, D.M., Luterman, A., Yurt, R.W., Goodwin, C.W., and Hansborough, J. (2003). Clinical effects of inhibiting leukocyte adhesion with monoclonal antibody to intercellular adhesion molecule-1 (enlimomab) in the treatment of partial-thickness burn injury. J. Trauma *54*, 950–958.

Mitsiades, C.S., Mitsiades, N.S., Bronson, R.T., Chauhan, D., Munshi, N., Treon, S.P., Maxwell, C.A., Pilarski, L., Hideshima, T., Hoffman, R.M., and Anderson, K.C. (2003). Fluorescence imaging of multiple myeloma cells in a clinically relevant SCID/NOD in vivo model: biologic and clinical implications. Cancer Res. *63*, 6689–6696.

Musolino, A., Naldi, N., Bortesi, B., Pezzuolo, D., Capelletti, M., Missale, G., Laccabue, D., Zerbini, A., Camisa, R., Bisagni, G., et al. (2008). Immunoglobulin G fragment C receptor polymorphisms and clinical efficacy of trastuzumab-based therapy in patients with HER-2/neu-positive metastatic breast cancer. J. Clin. Oncol. *26*, 1789–1796.

Nimmerjahn, F., Bruhns, P., Horiuchi, K., and Ravetch, J.V. (2005). FcgammaRIV: a novel FcR with distinct IgG subclass specificity. Immunity *23*, 41–51.

Park, S., Jiang, Z., Mortenson, E.D., Deng, L., Radkevich-Brown, O., Yang, X., Sattar, H., Wang, Y., Brown, N.K., Greene, M., et al. (2010). The therapeutic effect of anti-HER2/neu antibody depends on both innate and adaptive immunity. Cancer Cell *18*, 160–170.

Rawstron, A.C., Orfao, A., Beksac, M., Bezdickova, L., Brooimans, R.A., Bumbea, H., Dalva, K., Fuhler, G., Gratama, J., Hose, D., et al.; European Myeloma Network. (2008). Report of the European Myeloma Network on multiparametric flow cytometry in multiple myeloma and related disorders. Haematologica *93*, 431–438.

Richardson, P.G., Lonial, S., Jakubowiak, A.J., Harousseau, J.L., and Anderson, K.C. (2011). Monoclonal antibodies in the treatment of multiple myeloma. Br. J. Haematol. Published online July 21, 2011. http://dx.doi.org/10.1111/j.1365-2141.2011.08790.

Sampaio, M.S., Vettore, A.L., Yamamoto, M., Chauffaille, Mde.L., Zago, M.A., and Colleoni, G.W. (2009). Expression of eight genes of nuclear factor-kappa B pathway in multiple myeloma using bone marrow aspirates obtained at diagnosis. Histol. Histopathol. *24*, 991–997.

Schmidmaier, R., Baumann, P., Simsek, M., Dayyani, F., Emmerich, B., and Meinhardt, G. (2004). The HMG-CoA reductase inhibitor simvastatin overcomes cell adhesion-mediated drug resistance in multiple myeloma by geranylgeranylation of Rho protein and activation of Rho kinase. Blood *104*, 1825–1832.

Schmidmaier, R., Mörsdorf, K., Baumann, P., Emmerich, B., and Meinhardt, G. (2006). Evidence for cell adhesion-mediated drug resistance of multiple myeloma cells in vivo. Int. J. Biol. Markers *21*, 218–222.

Schneider, D., Berrouschot, J., Brandt, T., Hacke, W., Ferbert, A., Norris, S.H., Polmar, S.H., and Schäfer, E. (1998). Safety, pharmacokinetics and biological activity of enlimomab (anti-ICAM-1 antibody): an open-label, dose escalation study in patients hospitalized for acute stroke. Eur. Neurol. *40*, 78–83.

Smith, M.R. (2003). Rituximab (monoclonal anti-CD20 antibody): mechanisms of action and resistance. Oncogene *22*, 7359–7368.

Söderlind, E., Strandberg, L., Jirholt, P., Kobayashi, N., Alexeiva, V., Aberg, A.M., Nilsson, A., Jansson, B., Ohlin, M., Wingren, C., et al. (2000). Recombining germline-derived CDR sequences for creating diverse single-framework antibody libraries. Nat. Biotechnol. *18*, 852–856.

Stebbings, R., Findlay, L., Edwards, C., Eastwood, D., Bird, C., North, D., Mistry, Y., Dilger, P., Liefooghe, E., Cludts, I., et al. (2007). "Cytokine storm" in the phase I trial of monoclonal antibody TGN1412: better understanding the causes to improve preclinical testing of immunotherapeutics. J. Immunol. *179*, 3325–3331.

van der Kolk, L.E., Grillo-López, A.J., Baars, J.W., Hack, C.E., and van Oers, M.H. (2001). Complement activation plays a key role in the side-effects of rituximab treatment. Br. J. Haematol. *115*, 807–811.

Weiner, L.M., Surana, R., and Wang, S. (2010). Monoclonal antibodies: versatile platforms for cancer immunotherapy. Nat. Rev. Immunol. *10*, 317–327.

Weng, W.K., and Levy, R. (2003). Two immunoglobulin G fragment C receptor polymorphisms independently predict response to rituximab in patients with follicular lymphoma. J. Clin. Oncol. *21*, 3940–3947.

Wilson, N.S., Yang, B., Yang, A., Loeser, S., Marsters, S., Lawrence, D., Li, Y., Pitti, R., Totpal, K., Yee, S., et al. (2011). An Fcγ receptor-dependent mechanism drives antibody-mediated target-receptor signaling in cancer cells. Cancer Cell *19*, 101–113.

Yaccoby, S., Barlogie, B., and Epstein, J. (1998). Primary myeloma cells growing in SCID-hu mice: a model for studying the biology and treatment of myeloma and its manifestations. Blood *92*, 2908–2913.

Zhang, W., Gordon, M., Schultheis, A.M., Yang, D.Y., Nagashima, F., Azuma, M., Chang, H.M., Borucka, E., Lurje, G., Sherrod, A.E., et al. (2007). FCGR2A and FCGR3A polymorphisms associated with clinical outcome of epidermal growth factor receptor expressing metastatic colorectal cancer patients treated with single-agent cetuximab. J. Clin. Oncol. *25*, 3712–3718.

Zheng, Y., Cai, Z., Wang, S., Zhang, X., Qian, J., Hong, S., Li, H., Wang, M., Yang, J., and Yi, Q. (2009). Macrophages are an abundant component of myeloma microenvironment and protect myeloma cells from chemotherapy drug-induced apoptosis. Blood *114*, 3625–3628.

Zheng, Y., Yang, J., Qian, J., Qiu, P., Hanabuchi, S., Lu, Y., Wang, Z., Liu, Z., Li, H., He, J., et al. (2012). PSGL-1/selectin and ICAM-1/CD18 interactions are involved in macrophage-induced drug resistance in myeloma. Leukemia. Published online September 21, 2012. http://dx.doi.org/10.1038/leu.2012.272.